ISSN 1063-7850, Technical Physics Letters, 2014, Vol. 40, No. 11, pp. 1000–1002. © Pleiades Publishing, Ltd., 2014.
Original Russian Text © S.M. Peshcherova, A.I. Nepomnyashchikh, L.A. Pavlova, 2014, published in Pis'ma v Zhurnal Tekhnicheskoi Fiziki, 2014, Vol. 40, No. 22, pp. 30–36.

The Electric Activity of Special Grain Boundaries in Multicrystalline Silicon Grown from Metallurgical Refined Silicon

S. M. Peshcherova*, A. I. Nepomnyashchikh, and L. A. Pavlova
Vinogradov Institute of Geochemistry, Siberian Branch, Russian Academy of Sciences, Irkutsk, 664033 Russia
**e-mail: spescherova@mail.ru*

Received July 15, 2014

Abstract—The properties of special grain boundaries in multicrystalline silicon (mc-Si) grown from metallurgical refined silicon by the Bridgman–Stockbarger method have been studied. The electric activity of grain boundaries was characterized by measuring the electron-beam-induced current. Structural features of the mc-Si samples were studied by scanning electron microscopy, electron-probe microanalysis, and atomic force microscopy techniques.

DOI: 10.1134/S106378501411025X

Multicrystalline silicon (mc-Si) growth from metallurgical refined silicon is a promising material for solar power engineering. The advantages of mc-Si include low cost and relative simplicity of production in comparison to the material obtained from scrap for microelectronics. It should be noted that impurities that are present in metallurgical silicon strongly influence the formation of the macro- and microstructure of mc-Si [1–3]. In the course of crystallization, these impurities actively interact with various defects of the silicon structure and form additional centers of recombination of nonequilibrium charge carriers (NCCs). Numerous investigations were devoted to the effect of impurities on the electrical properties of extended defects in silicon [4–12]. However, no commonly accepted opinion about the electric activity of special grain boundaries (SGBs), which are the most frequently encountered defects in mc-Si, have been formulated so far. Therefore, further investigation of the properties of SGBs in mc-Si is topical, both for optimization of the technology of high-quality material for solar power engineering and for deeper insight into some fundamental issues of the physics of semiconductors.

The present work has been devoted to studying the structural and electric properties of SGBs in mc-Si grown by the Bridgman–Stockbarger method from metallurgical refined silicon.

The experiments were performed with samples prepared from transverse cut mc-Si ingots grown by the Bridgman–Stockbarger method, with largest grans containing twin lamellae. The sample surface was mechanically ground by diamond pastes and chemically polished by a mixture of HF and HNO_3 acids. The distribution of NCC recombination rate was determined by the method of electron-beam-induced current (EBIC) on the samples with Schottky barriers formed by the vacuum deposition of aluminum contacts. The structure and chemical composition of samples, from which the oxidized surface layer was removed by grinding with diamond pastes and chemical polishing with HF, were studied by electron-probe microanalysis (EPMA) and electron backscatter diffraction (EBSD) techniques.

It was previously established [13] that most large grains in mc-Si, with cross-sectional dimensions up to several centimeters, contain twin lamellae and exhibit short NCC lifetimes. However, a decrease in the NCC lifetime was observed not in all large grains with twin lamellae. Figure 1 presents the results of EBIC measurements of the spatial distribution of NCC recombination rate over the surface of mc-Si samples and the data of their structural characterization by the methods of atomic force microscopy (AFM) and EBSD. As can be seen from Fig. 1a, electric activity is inherent in all random-type grain boundaries (RGBs) and second-order twin grain boundaries ($\Sigma3$-GBs) in region *2*. It should be noted that $\Sigma3$-GBs are also present in the adjacent region *1*, but these boundaries are electrically inactive. Since the surface of silicon prior to Al deposition was chemically etched for several seconds according to the procedure of sample preparation to EBIC measurements, this surface was optically smooth. The AFM data obtained at large magnification (Fig. 1b) show that the surface relief in region *1* (Fig. 1a) exhibits straight lines oriented at various angles. At the same time, the surface in region *2* contains globular particles situated along lines analogous to those in region *1* (Fig. 1d). Differences in the surface texture of neighboring regions *1* and *2* revealed by the etching are indicative of a difference in structures of the corresponding grains. Indeed, according to

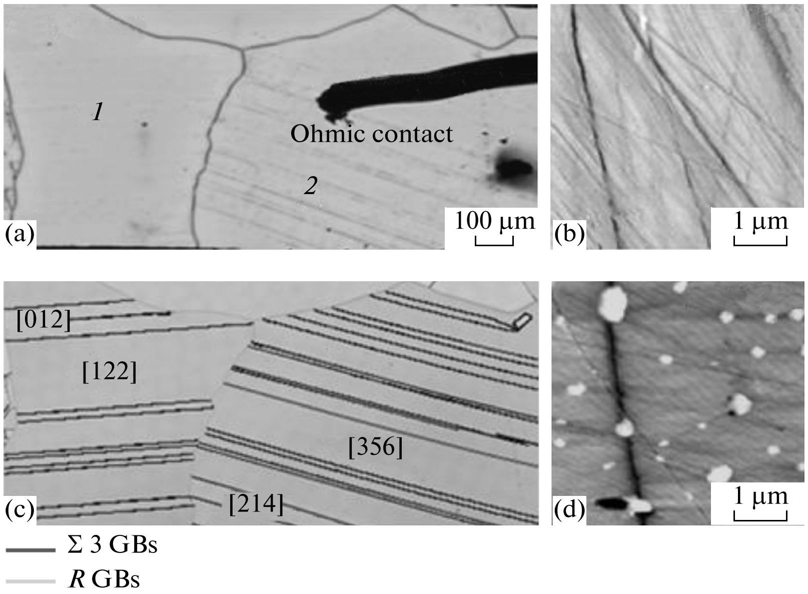

Fig. 1. Results of investigation of the surface of mc-Si: (a) map of the spatial distribution of NCC recombination rate by EBIC data; (b, d) AFM images of the sample surface in regions *1* and *2* indicated in (a); (c) map of SGB distribution by EBSD data.

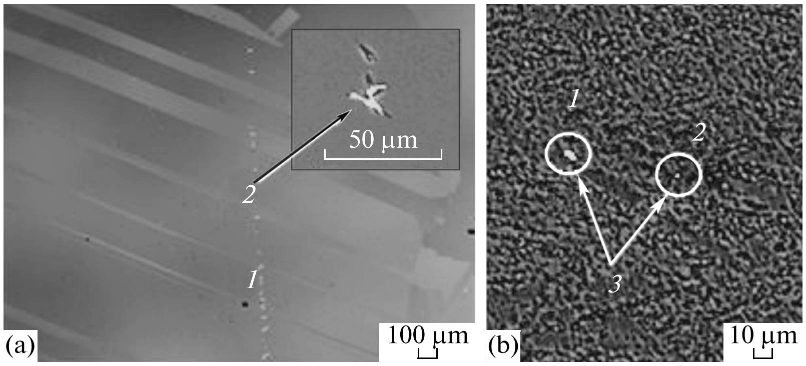

Fig. 2. EPMA images of region *2* in backscattered electrons: (a) ground surface; (b) etched surface.

EBSD data (Fig. 1c), region *1* comprises parent [122] grain and [012] twins, while region *2* includes parent [356] grain with [214] twins. Since the reticular atomic density (number of atoms per unit area) is inversely proportional to the Miller indices, the chemical bonds in region *2* are weaker and the corresponding interatomic distances are longer than in region *1*. Therefore, during crystallization, impurities were more effectively trapped and localized on extended defects in region *2*.

Thus, the electric activity of special Σ3-GBs is related to the concentration of microdefects and impurities in regions *1* and *2* (Fig. 1a). Investigation of the distribution of impurities in region *2* confirmed the assumption about increased number of microinclusions in this region. Figure 2 shows the results of EPMA analysis of the ground and etched surface in region *2*. The sample surface was treated with selective SR4-A etchant for 5 s at room temperature.

The observed band of electrically active defects (Fig. 1a) represents an accumulation of large (up to 20 μm) microinclusions. The elemental compositions of microinclusions arranged along the band are identi-

Elemental composition (mass %) of microinclusions (indicated in Fig. 2) on the mc-Si surface

Microinclusion	Si	O	C	Cr	Fe	Cu	S
a-1	28.3	26.7	25.8	19.2	0	0	0
a-2	29.9	21.6	37.7	10.8	0	0	0
b-1	96.4	0	0	1.3	2.3	0	0
b-2	98.7	0	0	0	0	1.1	0.2

cal (see table). Figure 2b shows an image of the surface of region *2* upon etching, which reveals numerous etch pits and grooves appearing as intersecting bands. Although most impurities were removed by etching, it is clearly seen that rare retained microinclusions (see table) occur inside the bands. This fact suggests that the bands represent extended defects formed during crystallization as energetically favorable positions for precipitation. These bands cross the mc-Si grains in various directions at certain angles relative to each other. Most probably, these bands are the projections of shear planes and give evidence of the presence of edge dislocations in the volume of mc-Si grains. It should be noted that shear bands as such are not the electrically active defects, which can be seen in Fig. 1a. However, they can exhibit electric activity at precipitation sites, such as in region *2*. Note also that the band of chromium precipitates in region *2* exhibited significant activity according to EBIC data. After chemical etching of the aluminum mask and mechanical grinding of the surface (to a depth of about 100 μm from the initial surface), we could still study this defect by EPMA. From this it follows that shear bands with chromium precipitates, as well as other shear bands observed on the surface, are present in the grain volume.

The crystallization of mc-Si from metallurgical refined silicon by the Bridgman–Stockbarger method leads to the formation of ingot with predominantly coarse-block macrostructure. A large fraction of coarse grains in mc-Si contain twin boundaries, more than 90% of which belong to Σ3-GBs. Depending on the crystallization conditions, the initial concentration of impurities in metallurgical refined silicon, and the crystallographic orientation of a growing grain, the same defects can exhibit differing electric activity. It is established that the crystallographic parameters of grains significantly influence peculiarities of the structure formed during crystallization. In particular, grains with large Miller indices possess lower reticular densities than those of grains with small indices, which implies that the rate of crystallization in the former case is higher and the crystallization surface is atomically rough. Despite the fact that grains can have large dimensions and contain electrically low active Σ3-GBs, their electric properties depend primarily on the crystallographic orientation. Since defects of the same type can differently influence the transport of charge carriers, it is important to know the positions of these defects in the structure of ingot and take into account the aforementioned factors in selecting optimum conditions for mc-Si crystallization by the Bridgman–Stockbarger method.

Acknowledgments. We are grateful to Prof. E.B. Yakimov and O.V. Feklisova (Institute for Problems of Microelectronic Technology, Chernogolovka) for conducting EBIC measurements and to S.S. Kolesnikov (Tekhnopark, Irkutsk State Technical University) for conducting EBSD measurements. The main results of this study were obtained based on facilities of the Baikal Analytical Center (Siberian Branch of the Russian Academy of Sciences).

REFERENCES

1. S. M. Peshcherova, A. I. Nepomnyashchikh, V. A. Bychinskii, L. A. Pavlova, and Yu. V. Sokol'nikova, Materialovedenie, No. 6, 52 (2013).
2. A. I. Nepomnyashchikh, R. V. Presnyakov, I. A. Eliseev, and Yu. V. Sokol'nikova, Tech. Phys. Lett. **37** (8), 739 (2011).
3. S. M. Peshcherova, L. A. Pavlova, A. I. Nepomnyashchikh, I. A. Eliseev, and Yu. V. Sokol'nikova, Izv. Vyssh. Ucheb. Zaved.: Mater. Elektron. Tekh., No. 4, 12 (2012).
4. J. Chen, T. Sekiguchi, R. Xie, P. Ahmet, T. Chicyo, D. Yang, S. Ito, and F. Yin, Scr. Mater. **52**, 1211 (2005).
5. J. Bailey, S. A. McHugo, H. Hieslmair, and E. R. Weber, J. Electron. Mater. **25**, 1417 (1996).
6. S. A. McHugo, J. Bailey, H. Hieslmair, and E. R. Weber, *Proceedings of the 24th IEEE Photovoltaic Specialist Conference (1994)*, Vol. 2, pp. 1607–1610.
7. S. A. McHugo, H. Hieslmair, and E. R. Weber, Appl. Phys. A **64**, 127 (1997).
8. E. R. Weber, Appl. Phys. A **30**, 1 (1983).
9. J. R. Davis, A. Rohatgi, R. H. Hopkins, P. D. Blais, P. Rai-Choudhury, J. R. McCormic, and H. C. Mollenkopf, IEEE Trans. Electron. Dev. **ED-27**, 677 (1980).
10. R. H. Hopkins and A. Rohatgi, J. Cryst. Growth **75**, 67 (1985).
11. S. A. McHugo, Appl. Phys. Lett. **71**, 1984 (1997).
12. A. Voight, C. Hassler, D. Karg, H. P. Strunk, G. Pensl, and M. Schulz, Solid State Phenom. **51–52**, 497 (1996).
13. S. M. Peshcherova, A. I. Nepomnyashchikh, L. A. Pavlova, I. A. Eliseev, and R. V. Presnyakov, Semiconductors **48** (4), 476 (2014).

Translated by P. Pozdeev